Molecular Details of Ovalbumin−Pectin Complexes at the Air/Water Interface: A Spectroscopic Study

Elena V. Kudryashova,[†,‡] Antonie J. W. G. Visser,[§,||,⊥] Arie van Hoek,[§] and Harmen H. J. de Jongh*[,†,#]

Wageningen Centre for Food Sciences/TI Food and Nutrition, P.O. Box 557, 6700 AN, Wageningen, The Netherlands, Division of Chemical Enzymology, Chemistry Department, Moscow State University, 119899 Moscow, Russia, Laboratory of Biochemistry and Biophysics, Wageningen University, Dreijenlaan 3, 6703 HA, Wageningen, The Netherlands, MicroSpectroscopy Centre, P.O. Box 8128, 6700 ET, Wageningen, The Netherlands, Department of Structural Biology, Faculty of Earth and Life Sciences, Vrije Universiteit Amsterdam, De Boelelaan 1087, 1081 HV, Amsterdam, The Netherlands, and TNO Quality of Life, Utrechtseweg 48, Zeist, The Netherlands

Received February 9, 2007. In Final Form: May 7, 2007

To stabilize air−water interfaces, as in foams, the adsorption of surface-active components is a prerequisite. An approach to controlling the surface activity of proteins is noncovalent complex formation with a polyelectrolyte in the bulk phase. The molecular properties of egg white ovalbumin in a complex with pectin in the bulk solution and at air/water interfaces were studied using drop tensiometry (ADT) and time-resolved fluorescence anisotropy techniques. The complex formation of ovalbumin with pectin in the bulk resulted in the formation of a compact structure with a different spatial arrangement depending on the protein/pectin ratio. Complex formation did not provide an altered protein structure, whereas the conformational stability was slightly increased in the complex. In excess pectin, an overall condensed complex structure is formed, whereas at limited pectin concentrations the structure of the complex is more "segmental". The characteristics of these structures did not depend on pH in the 7.0 to 4.5 regime. Interaction with pectin in the bulk solution resulted in a significantly slower adsorption of the protein to the air/water interface. The limited mobility of the protein at the interface was found for both ovalbumin and ovalbumin−pectin complexes. From both the rotational dynamics and total fluorescence properties of the protein in the absence and presence of pectin, it was suggested that the complex does not dissociate at the interface. Ovalbumin in the complex retains its initial "aqueous" microenvironment at the interface, whereas in the absence of pectin the microenvironment of the protein changed to a more nonpolar one. This work illustrates a more general property of polyelectrolytes, namely, the ability to retain a protein in its microenvironment. Insight into this property provides a new tool for better control of the surface activity of complex biopolymer systems.

Introduction

Biopolymers, such as proteins and polysaccharides, are known to play an important role in the formation and stabilization of films, foams, and emulsions both in biological and in artificial colloidal systems. Understanding biopolymer adsorption and molecular interactions at the interface in relation to the observed mesoscopic effects is therefore an important fundamental question with practical relevance. In the present work, the formation of a noncovalent complex of proteins with polyelectrolytes (PE) was studied as a possible approach to modulating the adsorption kinetics and the molecular properties of proteins at the air/water interface. To our knowledge, this is the first study where the molecular details of such complexes at interfaces have been presented.

Protein−PE complexes can be formed spontaneously in aqueous solution and are generally stable over a broad range of pH values as a result of the cooperative multipoint electrostatic interaction between oppositely charged groups on the protein and PE.[1−22] Depending on the protein/PE mixing ratio and the protein−PE binding affinity, one can obtain nonstoichiometric complexes in which most of the polyelectrolyte charges are noncompensated. Such complexes are colloidally stable and soluble in water. Alternatively, low solubility stoichiometric complexes can be obtained with no charge or a low net charge.[1−9]

* Corresponding author. E-mail: dejongh@tifn.nl. Tel: +31 317 486160. Fax: +31 317 485384.
[†] Wageningen Centre for Food Sciences/TI Food and Nutrition.
[‡] Moscow State University.
[§] Wageningen University.
[||] MicroSpectroscopy Centre.
[⊥] Vrije Universiteit Amsterdam.
[#] TNO Quality of Life.

(1) de Kruif, C. G.; Weinbreck, F.; de Vries, R. *Curr. Opin. Colloid Interface Sci.* **2004**, *9*, 340−349.
(2) Ganzevles, R. A.; Zinoviadou, K.; van Vliet, T.; Cohen Stuart, M. A.; de Jongh, H. H. J. *Langmuir* **2006**, *22*, 10089−10096.
(3) Ganzevles, R. A.; Cohen Stuart, M. A.; van Vliet, T.; de Jongh, H. H. J. *Food Hydrocolloids* **2006**, *20*, 872−878.
(4) Xia, J.; Dubbin, P. L. In *Macromolecular Complexes in Chemistry and Biology*; Dubbin, P. L., Bock, J., Davis, R. M., Schultz, D. N., Thies, C., Eds.; Springer: Berlin, 1994; pp 247−270.
(5) Kokufuta, E. In *Macromolecular Complexes in Chemistry and Biology*; Dubbin, P. L., Bock, J., Davis, R. M., Schultz, D. N., Thies, C., Eds.; Springer: Berlin, 1994; pp 301−324.
(6) Horn, D.; Heuck, C. C. *J. Biol. Chem.* **1983**, *258*, 1665−1670.
(7) Carlsson, F.; Malmsten, M.; Linse, P. *J. Am. Chem. Soc.* **2003**, *125*, 3140−3149.
(8) Matsunami, H.; Kikuchi, R.; Ogawa, K.; Kokufuta, E. *Colloids Surf., B* **2006**, 10.
(9) Kabanov, V. A.; Mustafaev, V. I. *Polym. Sci.* **1981**, *23A*, 255−260.
(10) Zelikin A. N.; Trukhanova, E. S.; Putnam, D.; Izumrudov, V. A.; Litmanovich, A. A. *J. Am. Chem. Soc.* **2003**, *125*, 13693−13699.
(11) Morozova, L.; Desmet, J.; Joniau, M. *Eur. J. Biochem.* **1993**, *218*, 303−309.
(12) Kudryashova, E. V.; Artemova, T. A.; Vinogradov, A. A.; Gladilin, A. K.; Mozhaev, V. V.; Levashov, A. V. *Protein Eng.* **2003**, *16*, 303−309.
(13) Kudryashova, E. V.; Gladilin, A. K.; Izumrudov, V. A.; van Hoek, A.; Visser, A. J. W. G.; Levashov, A. V. *Biochim. Biophys. Acta* **2001**, *1550*, 129−143.
(14) Mascotti, D. P.; Lohman, T. M. *Biochemistry* **1995**, *34*, 2908−2915.

10.1021/la700379m CCC: $37.00
Published on Web 06/22/2007

The dissociation constants (K_{diss}) found for such complexes are in the range of 1−200 base μM (per charge), depending on the nature of the polyelectrolyte and its degree of polymerization.[10−14] One could speculate that such complexes would not necessarily dissociate upon adsorption to a hydrophobic interface; they could even become more stable as a result of enhanced electrostatic interactions in media with lower dielectric constants. It has been demonstrated[7−9,13−15] that multipoint electrostatic interaction of a protein with a PE results in the formation of a condensed structure of the complex with a different spatial arrangement depending on the protein/PE ratio. Evidently, the formation of such structures could lead to large changes in the adsorption properties of the protein to, for example, air/water interfaces.

As described in detail elsewhere,[23−31] protein adsorption to air−water interfaces comprises a number of events. Consistent with this view, the following general features can be expected upon adsorption of protein/PE complexes compared to non-complexed protein: (i) slower diffusion to the interface due to a higher hydrodynamic volume of the complex;[2,3,8] (ii) longer lag times for the adsorption caused by the suppression of multimolecular interactions of the protein involved in the complex in the surface layer;[12,13,16,17] (iii) slower or more limited conformational changes at the interface due to the stabilization of the protein structure by interaction with PE;[11−13,16−19] and (iv) altered surface layer properties, such as thickness and density, that be also affected because of electrostatic repulsion, steric reasons, and a higher degree of hydration (characteristic of charged and polar polymers).[20−22] Recently, it was demonstrated that complex formation of β-lactoglobulin with pectin in the bulk affects both its adsorption kinetics at air/water interface as the stiffness of the adsorbed layer.[2,3]

Until now, however, there has been no information available on the precise molecular origin of the altered surface properties. In the present work, egg white ovalbumin (OVA) in complex with pectin was selected as a model for studying the properties of protein−PE complexes at the air−water interface. OVA is frequently used as a foam and emulsion stabilizing agent, whereas pectin is often employed for its bulk texturizing properties. The effect of complex formation on OVA adsorption kinetics at the air/water interface was monitored using automated drop tensiometry (ADT). This technique allows on-line monitoring of the development of surface pressure and provides an opportunity to determine surface rheological properties. (See, for example, ref 32.) To unravel the molecular origin of the observed surface rheological effects of complex formation, time-resolved fluorescence anisotropy (TRFA) was applied. Because of its high sensitivity and selectivity, this approach provides quantitative information on the dynamics, molecular interactions, and spatial arrangement of the fluorophore. As shown in a previous study,[13] this method is exceptionally informative when studying supramolecular assemblies. In TRFA experiments, both the total fluorescence and fluorescence anisotropy decays are monitored. The first yields the fluorescence lifetimes in the protein, providing information on the environment of the internal or external fluorophores. An analysis of the fluorescence anisotropy decay yields information on internal and overall rotational mobility in the protein and protein-containing complexes.[33,34] Previously, the formation of a quasi-regular compact structure of two levels (segmental and overall) in the complex of α-chymotrypsin with polymethacrylic acid was shown by TRFA experiments in which both the independent motion of the protein in the complex with PE segment and the overall motion of protein−PE complex were resolved.[13] More recently we have demonstrated that the TRFA technique can also be applied successfully in the reflection mode to monitor the behavior of the fluorophores specifically at the interface.[35,36] In this work, we demonstrate that TRFA, a powerful method for studying the supramolecular assemblies in bulk solution, being applied to interfacial studies, can provide new insights into the molecular mechanism behind the colloidal systems' formation and stabilization.

In this work, we aim to illustrate how this technique in combination with surface tension measurements allows one to reveal molecular details of the influence of noncovalent complex formation with pectin on the adsorption properties of ovalbumin at air/water interfaces. This knowledge should provide us with a better understanding how PEs can be used to modulate the protein behavior and molecular dynamics, which can be applied, for example, to control foam formation and stabilization. We believe that our approach can be considered to be a promising tool for the development of new colloidal systems with the desired functionality (i.e., for the food, pharmaceutical, and cosmetics industries).

Materials and Methods

Ovalbumin Purification. A batch of ovalbumin was purified from fresh hen eggs using the following semi-large-scale procedure based on published purification protocols.[37] From 9-day-old hen eggs, the egg white was separated from the yolk by hand. To the total egg white fraction (about 300 mL), 600 mL of a 50 mM Tris-HCl buffer at pH 7.5 containing 10 mM β-mercaptoethanol was added. This solution was stirred for 24 h at 4 °C. Subsequently, the solution was centrifuged for 30 min at 14 000*g* and 4 °C. The pellet was discarded, and 1800 mL of 50 mM Tris-HCl (pH 7.5) was added to the supernatant. After a 30 min period of gentle stirring, the solution was filtered over a paper filter (Schleicher & Schuell). To

(15) Cousin, F.; Gummel, J.; Ung, D.; Boue, F. *Langmuir* **2005**, *21*, 9675−9688.
(16) Kudryashova, E. V.; Gladilin, A. K.; Vakurov, A. V.; Levashov, A. V.; Heitz, F.; Mozhaev, V. V. *Biotechnol. Bioeng.* **1997**, *55*, 267−277.
(17) Sergeeva, V. S.; Efremenko, E. N.; Kazankov, G. M.; Glagilin, A. K.; Varfolomeev, S. D. *Biotechnol. Tech.* **1999**, *13*, 479−483.
(18) Burke, C. J.; Volkin, D. B.; Mach, H.; Middaugh, C. R. *Biochemistry* **1993**, *32*, 6419−6426.
(19) Gibson, T. D. *Dev. Biol. Stand.* **1996**, *87*, 207−217.
(20) Otamiri, M.; Adlercreutz, P.; Mattiasson, B. *Biocatalysis* **1992**, *6*, 291−305.
(21) Otamiri, M.; Adlercreutz, P.; Mattiasson, B. B. In *Biocatalysis in Non Conventional Media*; Tramper, J., Ed.; Elsevier Science Publishers: Amsterdam, 1992; pp 363−369.
(22) Izumrudov, V. A.; Kasaikin, V. A.; Zezin, A. V. *Polym. Sci.* **1976**, *18A*, 2488−2493.
(23) MacRitchie, F.; Alexander, A. E. *J. Colloid Interface Sci.* **1963**, *18*, 453−457.
(24) MacRitchie, F.; Alexander, A. E. *J. Colloid Interface Sci.* **1963**, *18*, 458−436.
(25) Graham, D. E.; Phillips, M. C. *J. Colloid Interface Sci.* **1979**, *70*, 403−414.
(26) Miller, R. *Colloids Surf., A* **2001**, *183*, 381−390.
(27) Narsimhan, G.; Uraizee, F. *Biotechnol. Progr.* **1992**, *8*, 187−196.
(28) Guzman, R. Z.; Carbonell, R. G.; Kilpatrick, P. K. *J. Colloid Interface Sci.* **1986**, *114*, 536−547.
(29) Eastoe, J.; Dalton, J. S. *Adv. Colloid Interface. Sci.* **2000**, *85*, 103−144.
(30) Damodaran, S.; Song, K. B. *Biochim. Biophys. Acta* **1988**, *954*, 253−264.
(31) de Jongh, H. H. J.; Kosters, H. A.; Kudryashova, E. V.; Meinders, M. B. J.; Trofimova, D.; Wierenga, P. A. *Biopolymers* **2004**, *74*, 131−135.
(32) Benjamins, J.; Cagna, A.; Lucassen-Reynders, E. N. *Colloids Surf., A* **1996**, *114*, 245−263.
(33) Brand, L.; Knutson, J. R.; Davenport, L.; Beechem, J. M.; Dale, R. E.; Walbridge, D. G.; Kowalczyk, A. A. Time-Resolved Fluorescence Spectroscopy: Some Applications of Associative Behavior to Studies of Proteins and Membranes. In *Spectroscopy and the Dynamics of Molecular Biological Systems*; Bayley, P. M., Dale, R. E., Eds.; Academic Press: London, 1985; pp 259−305.
(34) Lakowicz, J. R. *Principles of Fluorescence Spectroscopy*, 2nd ed.; Plenum Press: New York, 1999.
(35) Kudryashova, E. V.; Meinders, M. B. J.; Visser, A. J. W. G.; van Hoek, A.; de Jongh, H. H. J. *Eur. J. Biophys.* **2003**, *32*, 553−562.
(36) Kudryashova, E. V.; Visser, A. J. W. G.; de Jongh, H. H. J. *Protein Sci.* **2005**, *14*, 483−493.
(37) Kosters, H. A.; Broersen, K.; de Groot, J.; Simons, J. W. F. A.; Wierenga, P. A.; de Jongh, H. H. J. *Biotechnol. Bioeng.* **2003**, *84*, 61−70.

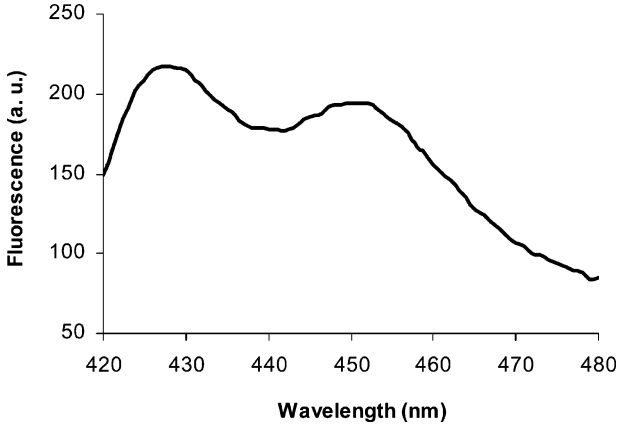

Figure 1. Fluorescence spectrum of OVA labeled with acridone 14 in 10 mM phosphate buffer (pH 7.0). The excitation wavelength is 390 nm.

the filtrate, 500 g of DEAE Sepharose Cl-6B (Pharmacia) was added, followed by overnight incubation at 4 °C under gentle stirring. Next, the solution was filtered over a glass filter (G2), followed by extensive washing with 10 L of demineralized water and 5 L of 0.1 M NaCl successively. The protein was eluted stepwise with subsequent steps of 1 L of 0.1, 0.15, 0.2, 0.25, and 0.35 M NaCl. The latter two eluents did contain some ovalbumin but appeared slightly yellowish and were discarded. The 0.15 and 0.2 M NaCl batches were pooled and concentrated using a Millipore ultrafiltration unit with a 30 kDa molecular mass cutoff membrane. The concentrated solution was dialyzed extensively against demineralized water, freeze dried, and stored at −40 °C until further use. The yield of this procedure is generally about 1.0 g of ovalbumin per egg, and the efficiency of isolation is over 90%. The purity of the protein was over 98% as estimated from a densitometric analysis of SDS-PAGE gels.

Pectin. Low methoxyl pectin was supplied by CP Kelco (Lille Skensved, Denmark). The degree of methylation is 30.4% (only the non-methylated galacturonic acid subunits have a free carboxyl group, pK_a ∼3.5), the uronic acid content is 78.5% (26), the averaged molecular weight (M_n) is 1.5×10^5 g/mol, and the polydispersity (M_w/M_n) is 2.4. Pectin solutions were prepared by wetting the powder with ethanol and subsequent dispersion in water, followed by heating to 70 °C for 30 min. After overnight stirring at 20 °C, the samples were centrifuged at 6000*g* for 10 min and stored at 4 °C until further use.

Labeling of Ovalbumin with the *N*-Hydroxysuccinimidyl Ester of Acridone 14. The *N*-hydroxysuccinimidyl ester of acridone 14[38] was supplied by Amersham Bioscience (U.K.). The labeling of ovalbumin with the *N*-hydroxysuccinimidyl ester of acridone 14 was carried out according to the Molecular Probes protocol for labeling proteins with amine-reactive probes (http://www.probes.com). Typically, 10 mg of ovalbumin was dissolved in 1 mL of 0.1 M sodium bicarbonate buffer (pH 8.3). A stock solution of acridone 14 *N*-hydroxysuccinimidyl ester (5 mg in 0.5 mL) was prepared in DMSO. While the protein solution was stirred, the reactive dye solution was added in several portions. The mixture was stirred for 1 h at room temperature. The reaction was terminated by the addition of 0.1 mL of 1.5 M hydroxylamine solution (pH 8.5). The conjugate was separated from the nonreacted reagent on a Sephadex G-25 gel filtration column (10×300 mm^2) equilibrated with 10 mM sodium phosphate buffer (pH 7.0). The degree of modification (N) was determined using the following equation: $N = A_{max}\mathrm{MW}/[\mathrm{protein}]\epsilon_{dye}$, where A_{max} is the absorbance of the protein−dye conjugate (Figure 1), MW is the molecular weight of the protein, ϵ_{dye} is the extinction coefficient of acridone 14 *N*-hydroxysuccinimidyl ester at its absorbance maximum (7190 M^{-1} cm^{-1} at 413 nm), and the protein concentration is expressed in mg/mL. The determined average degree of modification of ovalbumin was ∼1 mol of dye per mol of protein.

(38) Smith, J. A.; West, R. M.; Allen, M. *J. Fluoresc.* **2004**, *14*, 151−71.

Automated Drop Tensiometry (ADT) Experiments. An automated drop tensiometer (ADT, ICT, France) was used to measure the interfacial tension between the liquid and gas phases as a function of time. The setup is described in detail elsewhere.[32] The interfacial tension was determined by means of drop shape analysis of a bubble of air formed within a cuvette containing 0.05 mg/mL protein solution in 10 mM phosphate buffer at pH 7.0 or acetate buffer at pH 4.5. The bubble was illuminated by a light source, and its profile was imaged and digitized by a CCD camera and a computer. The profile was used to calculate the interfacial tension using Laplace's pressure equation. The temperature was kept constant at 22 (±1) °C. All curves were measured in duplicate from two different solutions. Between repetitions, the variation in surface pressure measured at certain times was within 3 mN/m.

Circular Dichroism Spectroscopy. For all circular dichroism (CD) experiments, a Jasco J715 spectropolarimeter thermostatted at 20 (±1) °C was used. Far-UV CD spectra of 0.1 mg/mL ovalbumin in the presence and absence of pectin in 10 mM phosphate buffer (pH 7.0) were recorded in the range from 190 to 260 nm with a spectral resolution of 0.2 nm. The scan speed was 100 nm/min, and the response time was 0.125 s with a bandwidth of 1 nm. Quartz cells with an optical path of 0.1 cm were used. Typically, 16 scans were accumulated and subsequently averaged. The spectra were corrected for the corresponding protein-free sample.

Guanidine Titration Studies. A 10 mM phosphate buffer solution at pH 7.0 was prepared using reagent grades salts KH_2PO_4 and K_2HPO_4 (Merck) in demineralized water, and an 8 M GdnHCl stock solution was prepared by dissolving 1.816 g of GdnHCl salt (Merck) per mL of buffer. The protein stock solutions were prepared by diluting the protein with phosphate buffer at approximately 1 mg/mL. The protein stock solution (100 μL) was then diluted in 2 mL of GdnHCl solution to final concentrations ranging from 0 to 6 M. The pH of each solution was controlled by pH-paper coloration and was found to be similar to the buffer pH. Prior to measurement, the samples were incubated for 2 h at room temperature, which was required to reach equilibrium (unpublished results). After incubation, the sample was poured into a thermostated 1 mL quartz cell. The fluorescence emission was recorded between 300 and 450 nm upon excitation at 274 and 295 nm on an LS 50 B luminescence spectrometer (Perkin-Elmer). The slit widths were set at 5 nm. The denaturation curves were obtained by plotting the band intensity at 335 for a fixed emission wavelength of 274 nm as a function of GdnHCl concentration.

Langmuir Trough Experiments. A Teflon Langmuir trough with two compartments for the sample and the reference was used to study the protein properties at the air/water interface. The dimensions of the Langmuir trough were 3×2.6 cm^2 (5 mL) and were equal for the sample and reference compartments. A pressure sensor connected to a paper Wilhelmy plate measured the surface pressure. Prior to any measurements, the film balance was calibrated using standard weights. The surface tension (σ_0) of the buffer solution in the reference compartment was 72.2 mN/m. Typically, 5 mL of a protein solution of 0.05 mg/mL in 10 mM phosphate buffer (pH 7.0, using Millipore water) was transferred to the sample compartment. All experiments were carried out at 22 °C.

TRFA Measurements. Time-resolved fluorescence measurements were carried out using mode-locked continuous wave lasers for excitation and time-correlated photon counting as the detection technique. The pump laser was a CW diode-pumped, frequency-doubled Nd:YVO_4 laser (Coherent Inc., Santa Clara, CA, model Verdi V10). The mode-locked laser was a titanium/sapphire laser (Coherent Inc., Santa Clara, CA, model Mira 900-D in fs mode), tuned to 780 nm. A pulse picker (APE GmbH, Berlin, Germany, model Pulse Select) was placed at the output of the titanium/sapphire laser, decreasing the repetition rate of excitation pulses to 3.8×10^6 pulses/s. The output of the pulse picker was directed toward a frequency doubler (Inrad Inc, Northvale, NJ, model 5-050 ultrafast harmonic generation system). For excitation, a sub-pJ maximum pulse energy was used; the wavelength was 390 nm, and the pulse duration was about 0.2 ps.

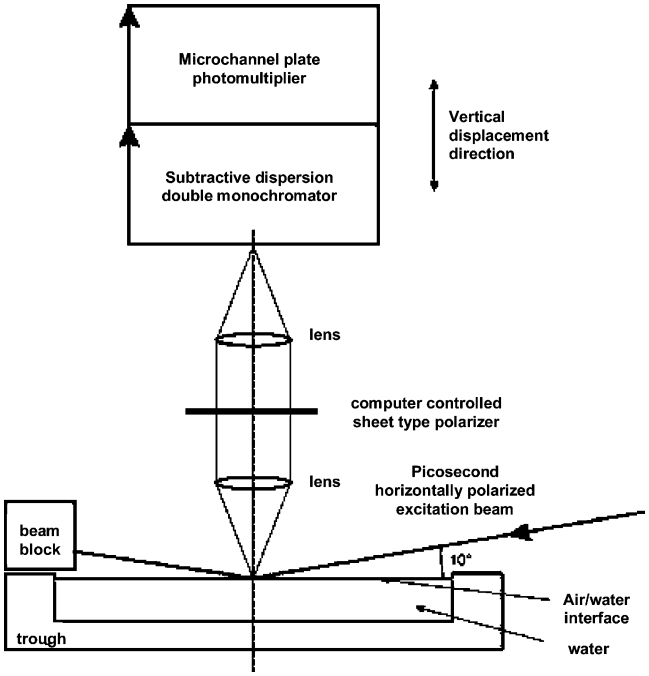

Figure 2. TRFA setup in external reflection mode combined with a Langmuir trough to measure the fluorescence properties of proteins at the air/water interface.

The samples were in 1 mL and 10 mm light path fused silica cuvettes (Hellma GmbH, Müllheim, Germany, model 111-QS); they were placed in a sample holder, and the temperature was controlled (20 °C) by applying thermoelectric (Peltier) elements and a controller (Marlow Industries Inc., Dallas, TX, model SE 5020). The fluorescence was collected at an angle of 90° with respect to the direction of the exciting light beam. The channel time spacing was 24.9 ps. By reducing the energy of the excitation pulses with neutral density filters, the rate of fluorescence of photons was decreased to less than 30 000/s (<1% of 3.8 MHz,[39]) to prevent pile-up distortion. Measurements consisted of repeated sequences of measurement during 10 s of parallel and 10 s of perpendicularly polarized emission. The number of sequences was chosen to yield a peak content in the data files of up to 100 000 counts. After the fluorescence of the sample was measured, the background emission of the buffer solution was measured and used for background subtraction. All curves were measured in duplicate from two different solutions. The variation in the lifetimes (τ_i) and correlation times (ϕ_i) obtained after an exhaustive error search (at the 67% confidence limit) in a global analysis of two separate experiments was within 10%. Pre-exponential factors are the average of two determinations and are accurate to the given digit.

For fluorescence and anisotropy lifetime measurements of the protein adsorbed at the air/water interface (in a Langmuir trough), the setup was slightly adapted for the external reflection mode (Figure 2). The polarization direction of the excitation beam was changed to horizontal, parallel to the plane of the interface; the beam was grazing the interface at 80° with respect to the normal. The direction of detection was vertical. After calibration of the optical system, TRFA measurements were performed as a function of adsorption time. For deconvolution purposes in the case of measurements at the Langmuir trough surface layer, the fluorescence decay of a fast reference compound was not used, but the scattered excitation light at that surface layer was used. The temperature of all experiments was 22 °C.

Fluorescence Intensity Decay Analysis. The total fluorescence intensity decay $I(t)$ is obtained from the measured parallel $I_{||}(t)$ and perpendicular $I_{\perp}(t)$ fluorescence intensity components relative to the direction of polarization of the exciting beam through the relation

$$I(t) = I_{||}(t) + 2I_{\perp}(t) \tag{1a}$$

for the bulk solution and

$$I(t) = I_{||}(t) + I_{\perp}(t) \tag{1b}$$

for the air/water interface.

The fluorescence lifetime profile consisting of a sum of discrete exponentials with lifetime τ_i and amplitude α_i can be retrieved from the total fluorescence $I(t)$ through the convolution product with the instrumental response function $E(t)$ according to

$$I(t) = E(t) \otimes \sum_{i=1}^{N} \alpha_i e^{-t/\tau_i} \tag{2}$$

Data analysis was performed with a model of discrete exponential terms as described before.[35,36] The TRFA Data Processing Package (version 1.2) of the Scientific Software Technologies Center (Belarusian State University, Minsk, Belarus; www.sstcenter.com)[40−42] was used.

Fluorescence Anisotropy Decay Analysis. In time-resolved fluorescence anisotropy experiments, the angular displacement of fluorophore emission dipoles is measured in real time. The experimental observable is the fluorescence anisotropy r defined as

$$r(t) = \frac{I_{||}(t) - I_{\perp}(t)}{I_{||}(t) - 2I_{\perp}(t)} \tag{3a}$$

for the bulk solution and

$$r(t) = \frac{I_{||}(t) - I_{\perp}(t)}{I_{||}(t) + I_{\perp}(t)} \tag{3b}$$

for the air/water interface.

The anisotropic decay of proteins is often affected by the rapid reorientation of the fluorophore in addition to the much slower overall rotation of the protein. This applies for both internal and external fluorophores attached to the protein. There is a simplified equation for the anisotropic decay of a protein exhibiting rapid internal reorientation and slow overall rotation[43]

$$r(t) = \left\{\beta_1 \exp\left(-\frac{t}{\phi_{\text{int}}}\right) + \beta_2\right\} \exp\left(-\frac{t}{\phi_{\text{prot}}}\right) \tag{4}$$

in which ϕ_{int} is the time constant for rapid internal reorientation, ϕ_{prot} is the rotational correlation time of the protein, and β_i is the relative contribution of the corresponding rotational correlation time to the decay. One can define a second-rank order parameter S for a fluorophore reorienting in a protein

$$S^2 = \frac{\beta_2}{\beta_1 + \beta_2} = \frac{1}{2}\cos\psi\,(\cos\psi + 1) \tag{5}$$

where $\beta_1 + \beta_2$ is the fundamental anisotropy (the anisotropy at time zero) and ψ is the angular displacement of the fluorophore due to internal reorientation. It can be seen that $S = 1$ when there is no internal flexibility ($\beta_1 = 0$), and the probe rotates together with the whole protein. The rate of reorientation is given by the diffusion coefficient $D_{\perp}$ of internal motion and can be calculated using ϕ_{int}:[44]

$$D_{\perp} = \frac{1 - S^2}{6\phi_{\text{int}}} \tag{6}$$

(39) Vos, K.; van Hoek, A.; Visser, A. J. *Eur. J. Biochem.* **1987**, *165*, 55−63.

(40) Borst, J. W.; Hink, M. A.; van Hoek, A.; Visser, A. J. W. G. *J. Fluoresc.* **2005**, *15*, 153−160.

(41) Novikov, E. G.; van Hoek, A.; Visser, A. J. W. G.; Hofstraat, J. W. *Opt. Commun.* **1999**, *166*, 189−198.

(42) Digris, A. V.; Skakun, V. V.; Novikov, E. G.; van Hoek, A.; Claiborne, A.; Visser, A. J. W. G. *Eur. Biophys. J.* **1999**, *28*, 526−531.

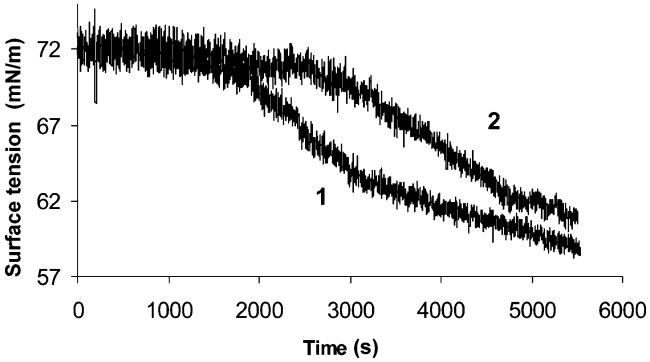

Figure 3. Monitoring the changes in the surface tension of free OVA (curve 1) and OVA−pectin complexes (OVA/pectin weight ratio of 10/1) (curve 2) using automated drop tensiometry (ADT). The surface tension is established by image analysis of the bubble projection as a function of time. The bulk protein concentration is 0.05 mg/mL in 10 mM phosphate buffer (pH 7.0).

The ϕ_{prot} value is related to the hydrodynamic radius of the particle, R_h, (or the total hydrodynamic volume, V_{tot}) via the Debye−Stokes−Einstein equation

$$\phi_{prot} = \frac{4\pi(R_h)^3\eta_v}{3kT} = \frac{\eta V_{tot}}{kT} \quad (7)$$

where k_B is the Boltzmann constant, T is the absolute temperature, and η_v is the viscosity of the medium. The molecular weight, MW, of the particle can be estimated, assuming that R_h is proportional to the cube root of MW. For the OVA−pectin complex, V_{tot} can be presented as

$$V_{tot} = V_{OVA} + V_{pectin} \quad (8)$$

where V_{OVA} is the volume of an OVA molecule (or its rotational segment) and V_{pectin} is the volume of a pectin molecule (or its section) bound to OVA.

Results and Discussion

Surface Tension. First, the influence of complex formation with pectin in the bulk on the ovalbumin (OVA) adsorption properties is studied by monitoring the effect on surface tension in time after generating a new air/water interface. Automated drop tensiometry (ADT) analysis was performed on samples of free OVA and (pre-equilibrated) OVA−pectin complexes of different OVA/pectin weight ratios to monitor the decrease in surface tension. Pectin by itself does not lower the surface tension (results not shown). Representative ADT curves for 0.05 mg/mL OVA in the absence and presence of pectin (at an OVA−pectin weight ratio of 10/1) at pH 7.0 are shown in Figure 3. Noncomplexed OVA shows at this concentration a lag time for adsorption (in the $\gamma-t$ curve) of about 1000 s, similar to that reported previously.[45,46] First, adsorption to the interface has to occur up to a typical surface load of 1 mg protein/m^2 before intermolecular interactions are so extensive that they lower the surface tension.[45] Depending on the OVA/pectin ratio, the lag time is affected by complex formation (Figure 4). Apparently, the maximal effect of pectin on the OVA adsorption rate is observed at high OVA/pectin ratios but not in excess pectin. At

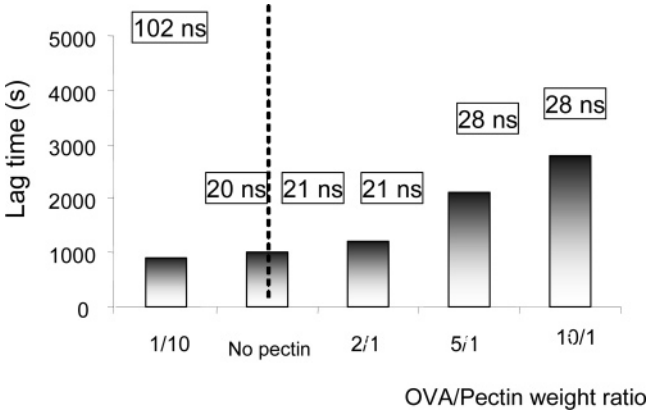

Figure 4. Lag time for adsorption of OVA in the complex with pectin measured by automated drop tensiometry (ADT) as a function of the OVA/pectin weight ratio. The corresponding rotational correlation times (ϕ_{long}, ns) determined by TRFA are indicated as well. The bulk protein concentration is 0.05 mg/mL in 10 mM phosphate buffer (pH 7.0).

OVA/pectin weight ratios of 5/1 and 10/1, the lag time for adsorption goes up to 2800 s, and the equilibrium surface tension (measured after prolonged incubation up to 10 000 s; not shown) is slightly higher (by 3 to 4 mN/m) compared to that for free OVA. The effect of pectin on the adsorption properties of OVA can be caused by slower diffusion to the interface expected for the OVA/pectin particles as a result of their considerable enlarged hydrodynamic volume compared to that of noncomplexed OVA. The hydrodynamic radius R_h found for the complex of another protein (β-lactoglobulin) with pectin of the same chain length is about 100 nm.[2,3] The R_h value of OVA itself is about 3.5 nm, as can be estimated using the diffusion coefficient $D = 6.0 \times 10^{-11}$ m^2/s determined elsewhere.[36,47] A second reason for the slower adsorption of the complex can be the suppression of multimolecular interactions of the protein at the interface due to the electrostatic repulsion of positively charged OVA−pectin complexes underneath the interface. At OVA/pectin weight ratios of 2/1 and 1/10 (the highest pectin concentrations studied), the lag time for protein adsorption is comparable to that in the absence of pectin. The increase in lag time and higher equilibrium surface tension observed for OVA/pectin at limited pectin concentration must thus be caused by the specific spatial arrangement of the complex and cannot be attributed to a slight increase in the viscosity of the system on pectin addition.

We have noticed that the lag time of OVA−pectin complexes is strongly dependent on the dielectric properties of the medium. The addition of ethanol (5−10%) substantially enhanced the effect of pectin,[48] whereas an increase in ionic strength diminished it. This is a clear indication that the main mechanism of the effect of pectin on OVA adsorption is via electrostatic complexation.

The results described above point to the formation of protein−PE complexes of different structure and stoichiometry depending on the protein/pectin ratio. One can speculate that with gradual enrichment of the pectin molecule with OVA a more condensed and rigid spatial arrangement of the complex is adopted, as proposed previously for other protein−polyelectrolyte complexes.[6−9,13−15,49] This is studied in the next sections.

(43) Szabo, A. *J. Chem. Phys.* **1984**, *81*, 150−167.
(44) Bastiaens, P. I.; Bonants, P. J. M.; van Hoek, A.; Muller, F.; Visser, A. J. W. G. Time-resolved fluorescence spectroscopy of NADPH-cytochrome P-450 reductase: demonstration of energy transfer between the two prosthetic groups. *Biochemistry* **1989**, *28*, 8416−8425.
(45) Razumovsky, L.; Damodaran, S. *Langmuir* **1999**, *15*, 1392−1399.
(46) Wierenga, P. A.; Meinders, M. B. J.; Egmond, M. R.; Voragen, A. G. J.; de Jongh, H. H. J. *Langmuir* **2003**, *19*, 850−857.
(47) Culbertson, C. T.; Jacobson, S. C.; Ramsey, J. M. *Talanta* **2002**, *56*, 365−373.
(48) Kudryashova, E. V.; de Jongh, H. H. J. Modulation of the adsorption properties of the complex of egg white ovalbumin with pectin by variation of the dielectric constant. To be submitted for publication.
(49) Izumrudov, V. A.; Margolin, A. L.; Zezin, A. V.; Kabanov, V. A. Properties of the non-stoichiometric complexes of globular proteins with polyelectrolytes. *Proc. Russ. Natl. Acad. Sci.* **1982**, *269*, 1508−1512.

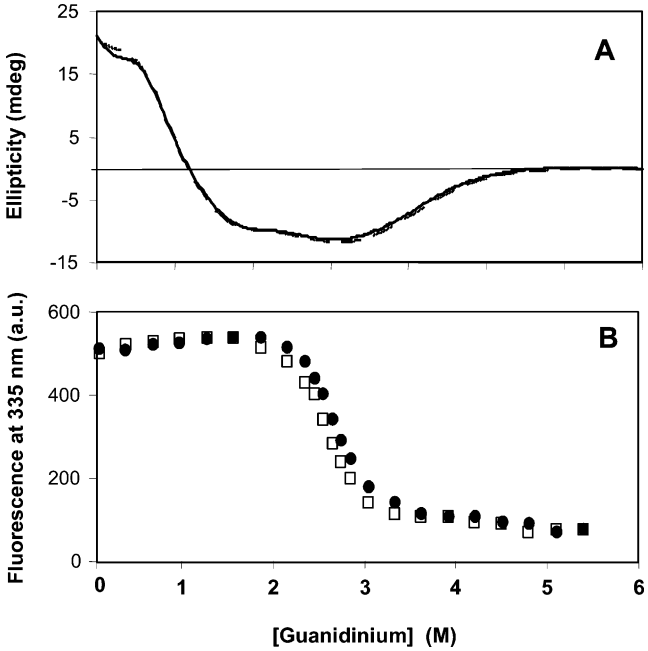

Figure 5. (A) Far-UV circular dichroism spectra of ovalbumin in the absence (−) and presence (---) of pectin at a protein/pectin ratio of 2/1. (B) Guanidinium titration of a 0.01 mg/mL ovalbumin solution (pH 7.0) in the absence (□) and presence (●) of pectin at a protein/pectin ratio of 2/1 as monitored by the fluorescence at 335 nm upon excitation at 274 nm.

Protein Structure and Stability in Complexes. From the above-described results, it can be suggested that in the bulk OVA induces the formation of certain spatial organization within the pectin molecule, whereas at the same time pectin affects the protein local environment (such as the hydration shell, local ion concentrations, local viscosity, and protein surface net charge). Because altered protein stability might affect the exerted surface pressure via the equation of state,[50] we first need to examine the consequences of complex formation on the protein structure and stability. For that purpose, circular dichroism was employed. From the far-UV CD spectra, shown in Figure 5A, it can be concluded that at ambient temperature no significant effect can be observed on the protein secondary structure upon addition of pectin in a 1/2 weight ratio. At other ratios used in this study, no spectral changes could be observed (not shown). To test the effect of complex fomation on protein stability, guanidinium titration studies were performed as shown in Figure 5B. Here it can be observed that at ambient temperature the titration curve of the monitored fluorescence intensity at 335 nm (emission maximum of the native protein) is shifted to slightly higher guanidinium concentrations, indicating higher stabilization energy for the protein in the presence of pectin. Assuming two-state unfolding for this protein, the presence of pectin increases the free energy from 28.1 (±0.6) to 29.8 (±0.7) kJ/mol. No effect of the protein/pectin ratio was found, suggesting that at the ratios tested all proteins were bound to pectin and that the charge stoichiometry between pectin and protein does not have an impact on the protein stability (results not shown). Stabilization of the structure of globular proteins by complexation with various polysaccharides under specific conditions has been reported.[51,52] These results indicate that it is not likely that the differences in adsorption properties derived from surface tension measurements are caused by differences in protein stability in the absence or presence of pectin.

TR Fluorescence and Rotational Dynamics of OVA and OVA−Pectin in the Bulk. To substantiate the suggested existence of a condensed spatial arrangement of OVA−pectin complexes, we have conducted studies using TRFA as a function of the OVA/pectin ratio. TRFA can be applied to evaluate the molecular dynamics and structural constraints of the protein−PE complexes at the air/water interface compared to those in the bulk solution. For TRFA experiments, OVA was labeled with acridone *N*-hydroxysuccinimidyl ester that has a fluorescence lifetime of 14.2 ns. The labeled protein did not show significantly different adsorption kinetics, as evidenced from surface pressure development in time or for the exerted equilibrium surface pressure (results not shown,[35]). In contrast to intrinsic tryptophan residues, this label is characterized by a long fluorescence lifetime allowing one to monitor relatively slow rotational motions expected for supramolecular structures such as protein/polyelectrolyte complexes (up to ∼100 ns). Examples of experimental and fitted total fluorescence and fluorescence anisotropy decays are shown in Figure 6 for OVA (A,B) and OVA−pectin complex at a weight ratio of 1/10 (C,D) in bulk solution. For OVA, the best fit to the experimental data of total fluorescence decay was obtained using a three-exponential function with a dominant long lifetime component, τ_3, of 14.1 ns (Table 1). The anisotropic decay of OVA exhibits rapid internal reorientation (characterized by a short correlation time ϕ_{int}) and slow overall rotation of the protein (characterized by a longer rotational correlation time ϕ_{long}). Table 1 summarizes the parameters obtained from the global analysis of the total fluorescence and fluorescence anisotropy decays for several OVA−pectin weight ratios. From these data, it can be deduced that upon complex formation with pectin the fluorescence lifetime distribution of OVA is practically unaffected whereas the rotational dynamics of OVA−pectin is changed significantly in a ratio-dependent manner (Table 1).

Noncomplexed OVA in bulk solution shows the rotational motion of a compact monomer. Its rotational correlation time (ϕ_{long} = 21.1 ns) is in good agreement with the value estimated for the globular protein of 45 kDa according to the Debye−Stokes−Einstein relation (eq 7). Similar ϕ_{long} values were obtained for OVA previously.[35,36] Complex formation with pectin in aqueous solution results in a slower anisotropic decay. Because the results presented in Figure 5 demonstrated that there are no indications for protein structural changes due to complex formation with pectin, the observed differences in anisotropy most likely reflect the binding of OVA to a pectin segment. Apparently, the size of such a segment depends on the protein/pectin ratio. With excess OVA (at OVA/pectin weight ratios of 10/1 and 2/1), the rotational correlation time (ϕ_{long}) increases from 21.1 to 28.1 ns. This ϕ_{long} value could be assigned to the rotational motion of an OVA molecule bound to a pectin segment with a MW of about 10 kDa (which is less than 10% of a whole pectin chain). This proposed structure of such a complex is schematically depicted in Figure 7A. One can suggest that in excess protein, complex formation induces the creation of segmental spatial arrangements in pectin. One pectin molecule is then composed of several segments characterized by independent motion, each containing a single bound OVA molecule. No rotational correlation time corresponds to the overall motion of the complex (or of several OVA molecules bound to different segments) at limited pectin concentration.

The situation looks different when pectin is present in excess. At an OVA/pectin weight ratio of 1/10, for example, the ϕ_{long}

(50) Wierenga, P. A.; Egmond, M. R.; Voragen, A. G. J.; de Jongh, H. H. J. *J. Colloid Interface Sci.* **2006**, *299*, 850−857.
(51) Burova, T. V.; Varfolomeeva, E. P.; Grinberg, V. Y.; Haertlé, T.; Tolstoguzov, V. B. *Macromol. Biosci.* **2002**, *2*, 286−292.
(52) Morozova, L.; Desmet, J.; Joniau, M. *Eur. J. Biochem.* **1993**, *218*, 303−309.

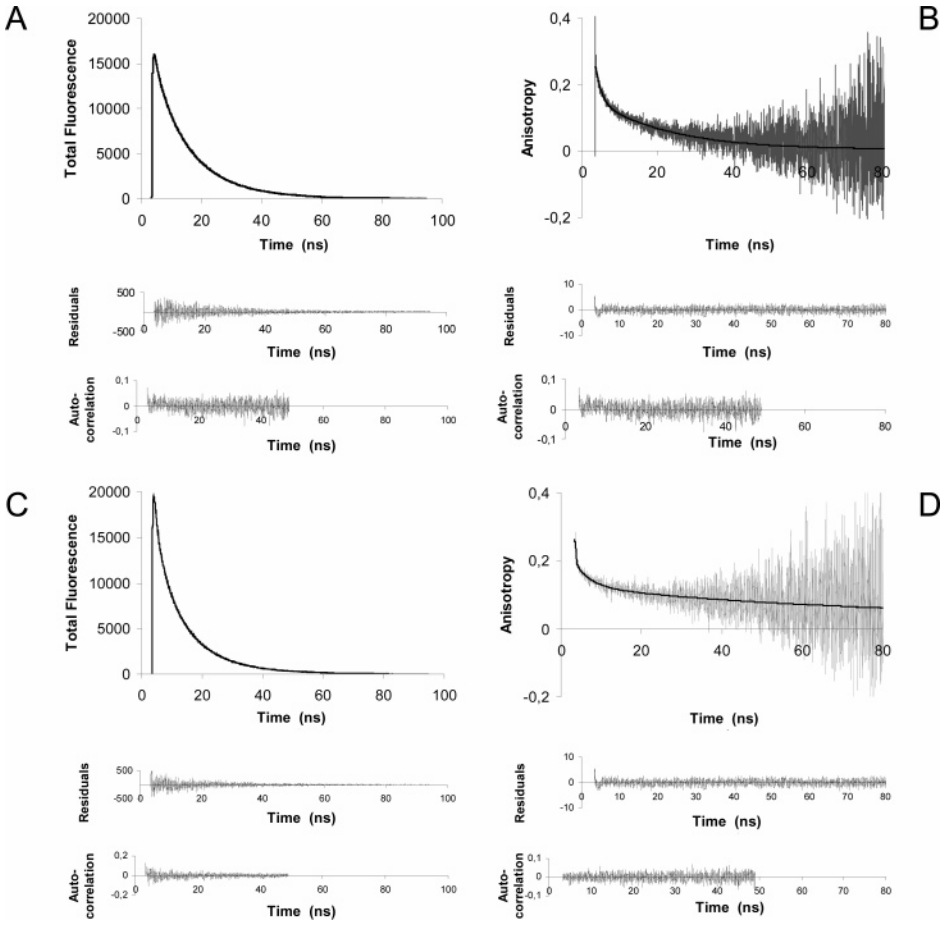

Figure 6. Total fluorescence and fluorescence anisotropy decays for (A, B) free OVA and (C, D) its OVA−pectin complex at an OVA/pectin weight ratio of 1/10 in the bulk solution. The bulk protein concentration is 0.05 mg/mL in 10 mM phosphate buffer (pH 7.0). Estimated fluorescence and anisotropic decay parameters are presented in Table 1.

Table 1. Estimated Total Fluorescence (α_i, τ_i) and Anisotropy Decay Parameters (β_i, ϕ_i, V_h, and $D_\perp$) of Ovalbumin and the OVA−Pectin Complex in the Bulk Solution and at the Interface (Int) at pH 7.0 (a) and pH 4.5 (b)[a]

OVA/pectin	β_1	ϕ_{int} (ns)[b]	β_2	$\phi_{2\ long}$ (ns)[b]	V_h (nm^3)	$D_\perp$ (ns^{-1})	α_1	τ_1 (ns)[c]	α_2	τ_2 (ns)[c]	α_3	τ_3 (ns)[c]
OVA	0.10	1.5	0.15	21.1	92.0	0.044	0.03	1.4	0.07	7.7	0.15	14.1
OVA/pectin 10/1	0.10	3.8	0.10	28.1	122.2	0.022	0.03	1.7	0.07	8.0	0.15	14.1
OVA/pectin 2/1	0.10	4.0	0.10	28.0	121.7	0.021	0.03	1.5	0.07	7.9	0.15	14.1
OVA/pectin1/1	0.10	1.3	0.15	20.4	88.7	0.051	0.03	1.6	0.07	8.2	0.15	14.2
OVA/pectin 1/2	0.10	1.6	0.15	21.6	93.9	0.042	0.03	1.5	0.07	7.8	0.15	14.1
OVA/pectin 1/10	0.10	4.2	0.12	101.7	422.2	0.018	0.1	1.2	0.1	6.2	0.15	13.5
Int OVA			0.10	5.1	22.2	0			0.04	4.0	0.10	13.0
Int OVA/pectin 10/1			0.10	10.8	47.0	0	0.03	2.5	0.05	7.1	0.15	13.5
Int OVA/pectin 1/10			0.10	9.6	41.7	0	0.03	2.1	0.05	7.1	0.15	13.5

[a] The excitation wavelength is 390 nm. [b] Rotational correlation times (ϕ_i) and their relative contributions (β_i) are defined by eq 4, the hydrodynamic volume (V_h) is defined by eqs 7 and 8, and the diffusion coefficient $D_\perp$ of internal motion is defined by eq 6. The variation in the lifetimes (τ_i) and correlation times (ϕ_i) obtained after an exhaustive error search (at the 67% confidence limit) was within 10%. [c] Fluorescence lifetimes (τ_i) and their relative contributions (α_i) are defined by eq 2.

value increases from 21 to ~102 ns. This long correlation time must be related to the rotational motion of the entire OVA−pectin complex with 1:1 stoichiometry (with a total MW of 165 kDa) rather than segments. According to the eq 7 for particles of such MW, a ϕ_{long} value of about 80−90 ns would be expected, which is in fairly good agreement with the experimental data. That the experimental ϕ_{long} value might even be higher than the expected value could point to the flexibility of the complex spatial arrangement. This can be due to the competition of charged groups in pectin (being largely in excess) for the positively charged binding sites on the protein surface. The proposed structure for the situation with excess pectin is schematically depicted in Figure 7B. At the same time, the higher degree of hydration within these complexes, as reported previously for proteins in complexes with a high polysaccharide content,[20,21] can also contribute to longer rotational correlation time ϕ_{long}. An increased degree of hydration within a complex leads to higher microviscosity of surrounding water molecules in the vicinity of a protein, a phenomenon that is known to damp rapid fluctuations in proteins.[53] This could also explain the slower label reorientation in the OVA−pectin complex: ϕ_{int} increases from 1.5 to about 4.2 ns upon complex formation (Table 1). According to eq 6, this corresponds to a decrease in the diffusion coefficient, $D_\perp$, of internal motion from 0.044 to 0.018 ns^{-1} (Table 1). Such an increase in

(53) Gavish, B; Werber, M. M. *Biochemistry* **1979**, *18*, 1269−1275.

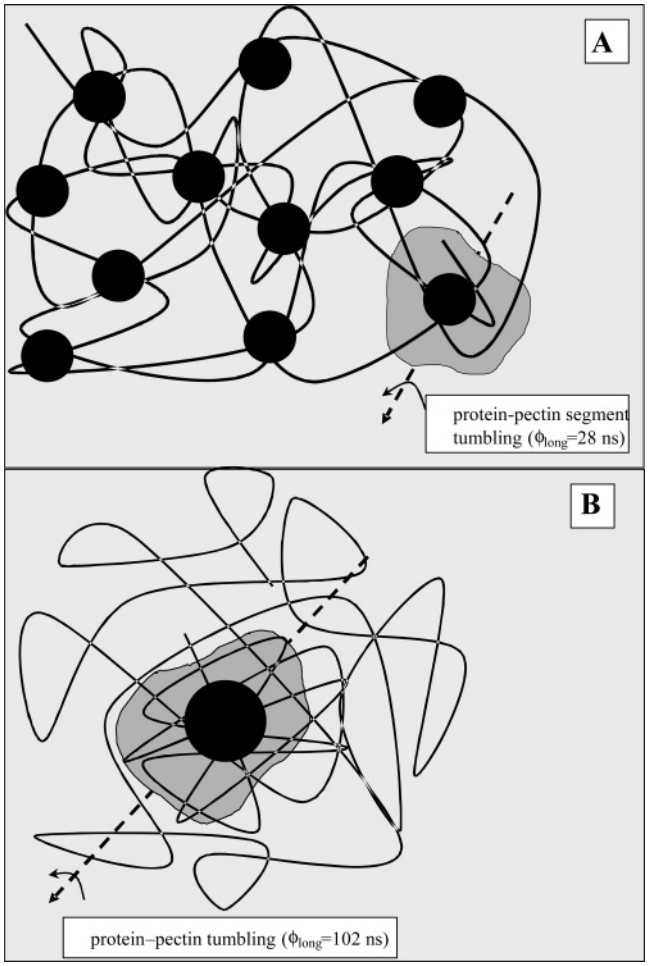

Figure 7. Schematic representation of OVA−pectin complexes in the bulk at (A) high and (B) low protein/pectin ratios.

microviscosity with increasing pectin content corresponds to the observed decrease in $D_\perp$ for the complexes with an OVA/pectin ratio that changes from 10/1 and 2/1 to 1/10 (Table 1).

At OVA/pectin ratios of 1/1 and 1/2, the rotational dynamics is practically unchanged upon addition of pectin (Table 1), indicating that OVA retains its independent rotational motion. The diffusion coefficient $D_\perp$ of internal motion is also retained (Table 1), assuming that the local microviscosity of the protein is not affected. This suggests that no specific spatial arrangement is formed at these OVA/pectin ratios (i.e., the structure of the complex is very flexible).

To observe whether pH would have a significant effect on the obtained complex configurations, similar experiments were performed at pH 4.5, where the protein has become slightly positive in net charge and pectin has become less negative because of the protonation of carboxylic groups on the protein surface (with pK_a's of ∼3.5). The TRFA results are summarized in Table 2 and show a comparable tendency as observed for pH 7.0 at all OVA/pectin ratios studied. It can therefore be concluded that complexes of analogous structure are formed in a broad pH interval independent of the net charge on the protein. Note that the total number of positive charges on the protein remains constant and that even some positive charges may become liberated from ion pairing when its carboxyl counterparts become protonated. The structure and stoichiometry of the complex depend primarily on the OVA/pectin ratio.

TR Fluorescence and Rotational Dynamics of OVA and OVA−Pectin Adsorbed at the Water/Air Interface. TRFA experiments performed at pH 7.0 in reflection mode show that the rotational correlation times of both OVA and OVA−pectin complex are much shorter at the interface compared to those in the bulk (Table 1). For example, in the absence of pectin the ϕ_{long} value of OVA decreases from 21.1 to 5.1 ns. Such a short rotational correlation time must arise from the motions of protein segments rather than overall protein motions. Apparently, large parts of the protein are immobilized at the interface (on the nanosecond time scale). This limited mobility of OVA at the interface was also shown previously.[35,36] At pH 4.5, the rotational correlation time of the protein at air−water interfaces is longer than at neutral pH but is still shorter than in the bulk (12.8 ns, Table 2). Apparently, OVA adsorbed at the interface exhibits different structural features compared to that at pH 7.0, despite the observation that the bulk characteristics were nearly equal (compare Tables 1 and 2). This might have to do with differences in unfolding kinetics at the interface that may cause differences in surface-area coverage.[50] The fluorescence lifetime distribution of noncomplexed OVA adsorbed at the interface is also different compared to that of bulk solution both at pH 7.0 and 4.5 (Tables 1 and 2). The total fluorescence decays are best fitted by a biexponential function with a dominant longer lifetime component, τ_3. The values of both τ_2 and τ_3 become shorter when the protein resides at the interface. These "interfacial" features of the fluorescence lifetime distribution of OVA remain constant with time of adsorption, as shown in Figure 8, and may reflect the change in environment of the label on the protein surface from a polar to a less polar one.

A different picture emerges for the adsorption of OVA in a complex with pectin assuming that protein−pectin complexes do not dissociate at the interface. At an OVA/pectin weight ratio of 10/1, adsorption of the complex to the interface leads to a decrease in the rotational correlation time ϕ_{long} to 10.8 ns. This ϕ_{long} does not change further with time of adsorption (up to 50 min, Figure 8). This correlation time can be assigned to the rotation of the protein segment in the complex with pectin. Assuming that independently of the OVA state (in the complex with pectin or not) the same segment of OVA retains its rotational mobility at the interface, the hydrodynamic volume of the pectin segment (V_{pectin}) bound to a single OVA molecule was calculated from ϕ_{long} values at the air/water interface in comparison with the bulk solution values (Table 1) using eqs 7 and 8. It can be read from the Table that at the interface the ratio V_{pectin}/V_{tot} is significantly higher (∼53%) compared to that in bulk solution (∼25%). We therefore conclude that at the interface the OVA−pectin complex adopts a more condensed state (i.e., a larger segment of pectin is bound to a single OVA molecule). This implies that more pectin binding sites are occupied in OVA and thus the efficiency of the interaction has increased. This can be the result of enhanced electrostatic interactions in an environment with a lower dielectric constant, as is the case at an interface.

Interestingly, a comparable spatial arrangement of OVA−pectin (with ϕ_{long} of ∼10 ns) is adopted at the interface independent of the initial OVA/pectin ratio of the complex (at OVA−pectin weight ratios of 1/10 and 10/1), despite the fact that the bulk ϕ_{long} values differed significantly (101.7 and 28.1 ns, respectively; Figure 8B). This result can be explained by the following consideration: adsorption of pectin in the noncomplexed form is unfavorable because of its polyelectrolyte properties, including a high degree of hydration and a noncompact structure,[3,6−8,20,21,49] providing a large entropic penalty upon adsorption. Apparently, the adsorption of pectin in complex with a protein proceeds much easier. This can be caused by the condensation of a pectin molecule, already lowering the entropy of the polyelectrolyte in the bulk effectively. Such condensation was recently observed

Table 2. Estimated Total Fluorescence (α_i, τ_i) and Anisotropy Decay Parameters (β_i, ϕ_i, V_h, and $D_\perp$) of Ovalbumin and the OVA−Pectin Complex in the Bulk Solution and at the Interface (Int) at pH 4.5[a]

OVA/pectin	β_1	ϕ_{int} (ns)[b]	β_2	$\phi_{2\ long}$ (ns)[b]	V_h (nm^3)	$D_\perp$ (ns^{-1})	α_1	τ_1 (ns)[c]	α_2	τ_2 (ns)[c]	α_3	τ_3 (ns)[c]
OVA	0.10	1.1	0.15	20.0	87.0	0.061	0.03	1.3	0.05	6.8	0.16	13.7
OVA/pectin 2/1	0.10	4.0	0.10	27.2	118.3	0.021	0.03	1.2	0.05	6.6	0.15	13.7
OVA/pectin 1/2	0.10	1.3	0.15	19.7	85.6	0.051	0.03	1.5	0.05	6.8	0.15	13.7
OVA/pectin 1/10	0.10	4.2	0.10	84.0	365.2	0.020	0.07	1.1	0.1	6.1	0.15	13.7
Int OVA			0.10	12.8	55.6	0			0.05	4.3	0.10	13.0
Int OVA/pectin 10/1			0.10	14.2	61.7	0	0.06	2.2	0.06	6.8	0.15	13.5

[a] The excitation wavelength is 390 nm. [b] Rotational correlation times (ϕ_i) and their relative contributions (β_i) are defined by eq 4, the hydrodynamic volume (V_h) is defined by eqs 7 and 8, and the diffusion coefficient $D_\perp$ of internal motion is defined by eq 6. The variation in the lifetimes (τ_i) and correlation times (ϕ_i) obtained after an exhaustive error search (at the 67% confidence limit) was within 10%. [c] Fluorescence lifetimes (τ_i) and their relative contributions (α_i) are defined by eq 2.

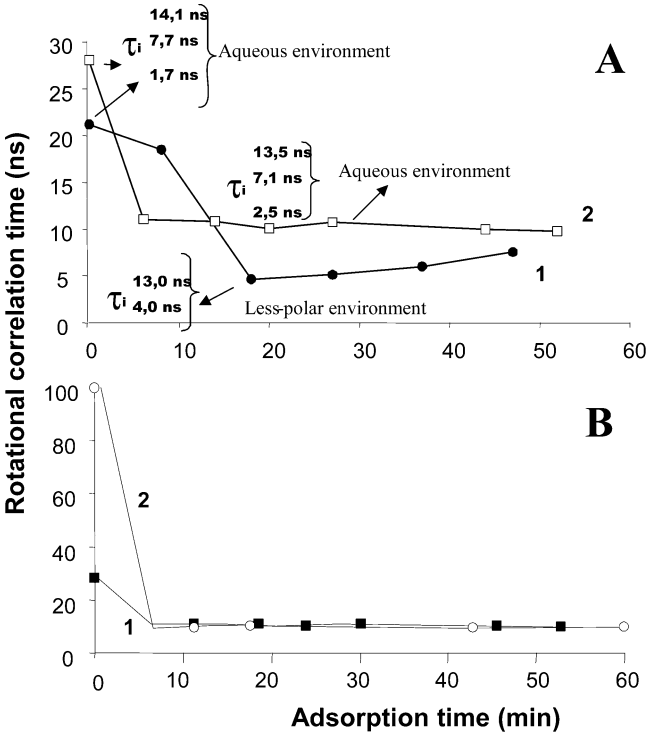

Figure 8. Rotational correlation times (ϕ_{long}, ns) as a function of adsorption time for OVA and OVA−pectin complexes obtained from TRFA experiments. (A) OVA (1): OVA−pectin complex with an OVA/pectin weight ratio of 10/1 (2). (B) OVA−pectin complexes: OVA/pectin weight ratios of (1) 10/1 and (2) 1/10. Fluorescence lifetime distributions (τ_i, ns) of OVA and OVA−pectin adsorbed at the air/water interface compared to the bulk solution (initial point) are indicated (A). The bulk protein concentration was 0.05 mg/mL in 10 mM phosphate buffer (pH 7.0).

elsewhere,[2] where it was reported that the hydrodynamic radius of the pectin molecule with the same degree of polymerization was reduced from 450 to about 100 nm upon complex formation with a β-lactoglobulin in the bulk. The compensation of the pectin charges upon the multipoint electrostatic interaction with OVA can also play a role in the facilitation of pectin adsorption. At an OVA/pectin weight ratio of 10/1 (corresponding to a charges ratio of approximately 1/1), the OVA−pectin complex is soluble in the bulk solution, indicating that there are a significant number of noncompensated charges in the complex. However, the majority of the pectin charges can be neutralized (with the formation of a "stoichiometric" complex) under conditions where electrostatic interactions are more effective. Such conditions are likely to be realized at the interface as a result of a decrease in the media polarity and the formation of the condensed and rather immobilized state of the complex. Alternatively, in the bulk solution the electrostatic interactions are less effective, making the structure of the complex more flexible. At an OVA/pectin weight ratio of 1/10 (charge ratios of ∼1/100) OVA−pectin complexes bear a high net negative charge; consequently, there is significant electrostatic repulsion between the particles that can suppress the formation of condensed layers at the interface. Consistent with this, only a limited amount of pectin can be accommodated at the interface under such conditions. The rearrangement of the spatial configuration of the complex toward the form where pectin is more saturated with OVA is required for effective adsorption. As a result of such rearrangement, the stoichiometric protein−pectin complex, in which polyelectrolyte charges are mostly compensated, is probably formed at OVA/pectin weight ratios of 1/10 and 10/1. We can suggest that the condensed and stoichiometric structure of the pectin−OVA complex is favorable at the interface and is formed independently at the initial OVA/pectin ratio (for a certain range of conditions). Excess pectin then could desorb to the bulk, whereas the ability to desorb the low-solubility stoichiometric OVA−pectin complex from the interface decreases.

Remarkably, in contrast to free OVA, the fluorescence lifetime distribution for OVA−pectin complexes is practically unchanged upon adsorption at both pH 4.5 and 7.0 (Figure 8A, Tables 1 and 2). This indicates that upon adsorption to the air/water interface, OVA in the complex with pectin retains its initial aqueous microenvironment whereas the environment of noncomplexed OVA has changed. Apparently, binding to pectin protects the protein from exposure to a less polar environment (such as the water−air interface) by the additional hydration shell around the protein provided by the polyelectrolyte. A similar effect of the polyelectrolyte on the protein was observed previously in water−organic solvent systems.[12,13]

In summary, the results presented in this work might be illustrative of a more general property of polyelectrolytes: complex formation with proteins provide these proteins with a higher stabilization of the initial conformation and with a microenvironment for the protein that better preserves its desired functional behavior, as, for example, enzyme activity or surface rheological behavior. In this way, the diversity of polyelectrolytes offers a very dedicated toolbox with which to optimize these properties because they vary significantly in molecular weight, charge density, and flexibility of the polyelectrolyte. This work demonstrates that these parameters can be used to influence the functional behavior of proteins at air/water interfaces because they determine the quality and quantity of the multipoint interactions with positive residues on proteins.

Acknowledgment. We greatly acknowledge Amersham Bioscience for providing us with the fluorescent label.

LA700379M